

Evaluation of Weld Defects in Petroleum Pipelines Using X-Ray for MAG, TIG, and SMAW Techniques

<http://www.doi.org/10.62341/hatr0553>

Hosam Almabruk Alnaily, Tariq Ramadan Aboalhol

The Libyan Higher Technical Center for Training and Production
Hosamalkaber1985@gmail.com

Abstract

The integrity of weld joints in petroleum pipelines is critical to ensuring the safe and efficient transport of fluids. This study evaluates the welding quality of pipes using Shielded Metal Arc Welding (SMAW), Gas Metal Arc Welding (MAG), and Gas Tungsten Arc Welding (TIG) methods. Thirty-six pipe samples were prepared and welded in the 6G position for each technique. X-ray computed tomography was employed to detect and analyze internal weld defects, adhering to ASME standards for acceptability. Defects such as porosity, incomplete penetration, and undercutting were identified, significantly impacting weld quality. Samples exhibiting major defects were rejected, while others met the acceptance criteria. The study underscores the necessity of advanced imaging techniques for accurate defect detection, thereby enhancing weld quality and reliability in pipeline applications. These findings provide valuable insights for improving welding practices, ultimately contributing to reliable and more efficient pipeline systems.

Keywords: weld defect evaluation, petroleum pipelines, X-Ray imaging, SMAW, MAG, TIG techniques.

تقييم عيوب اللحام في خطوط أنابيب البترول باستخدام الأشعة السينية لتقنيات MAG و TIG و SMAW

حسام المبروك النابلي، طارق رمضان أبو الهول

المركز الليبي التقني العالي للتدريب والإنتاج

Hosamalkaber1985@gmail.com

الملخص

يعتبر سلامة وصلات اللحام في خطوط أنابيب البترول أمراً بالغ الأهمية لضمان نقل السوائل بأمان وفعالية. تقيم هذه الدراسة جودة اللحام في الأنابيب باستخدام طرق اللحام بالقوس المعدني المحمي (SMAW) ولحام القوس الكهربائي باستخدام غاز تحجيب نشط (MAG) واللحام قوسي التنجستن والغاز الخامل (TIG) تم تحضير 36 عينة من الأنابيب ولحامها في موضع G6 لكل طريقة. تم استخدام التصوير المقطعي بالأشعة السينية (X-ray) لاكتشاف وتحليل عيوب اللحام الداخلية، وفقاً لمعايير القبول الخاصة بـ ASME. تم تحديد عيوب مثل المسامية والاختراق غير الكامل والتقيؤ، مما يؤثر بشكل كبير على جودة اللحام. تم رفض العينات التي تحتوي على عيوب كبيرة، بينما استوفت عينات أخرى معايير القبول. تؤكد الدراسة على ضرورة تقنيات التصوير المتقدمة للكشف الدقيق عن العيوب، مما يعزز جودة اللحام وموثوقيته في تطبيقات خطوط الأنابيب. توفر هذه النتائج رؤى قيمة لتحسين ممارسات اللحام، مما يساهم في الوصول لأنظمة أنابيب أكثر أماناً وكفاءة.

الكلمات المفتاحية: تقييم عيوب اللحام، خطوط أنابيب البترول، التصوير بالأشعة السينية، تقنيات SMAW، MAG، TIG.

Introduction

The evolution of welding techniques has significantly enhanced the safety, efficiency, and dependability of pipeline networks, which are essential for transporting fluids across industries like oil and gas. The integrity of weld joints in pipelines is important to prevent leaks, failures, and potential environmental hazards. Among the numerous welding techniques available, Shielded Metal Arc Welding (SMAW), Metal Active Gas Welding (MAG), and Tungsten Inert Gas Welding (TIG) are three predominant methods extensively employed in pipeline applications [1-5]. Each of these methods presents unique advantages and limitations that influence their suitability for different pipeline welding scenarios.

SMAW is well-known for its versatility and simplicity, making it a popular choice in field conditions where portability and ease of use are paramount. However, SMAW can be prone to defects such as slag inclusions and porosity if not executed with precision [6]. On the other hand, MAG offers higher deposition rates and cleaner welds with minimal post-weld cleanup, but the process demands more sophisticated equipment and a controlled environment to prevent contamination [7]. TIG stands out for its exceptional

precision and control, producing high-quality welds with minimal defects, albeit at a slower pace and higher cost compared to SMAW and MAG [8].

To ensure the integrity and reliability of weld joints, non-destructive testing (NDT) techniques are employed. Among these, X-ray imaging has emerged as a powerful tool for detecting internal defects such as cracks, voids, and impurities that are not visible to the naked eye. X-ray imaging allows for a comprehensive assessment of weld quality, providing important insights into the presence and extent of hidden defects [9]. The integration of advanced NDT methods like X-ray in pipeline welding evaluation enhances the overall safety and performance of pipeline systems, particularly in high-stakes industries like oil and gas [10].

In the oil and gas pipeline industry, electric arc welding methods such as SMAW, MAG, and TIG are the standard for pipe joining [11]. This sector is experiencing rapid growth, with expanded pipeline capacity through expansion loops and the construction of new pipelines to meet rising energy demands. These trends are driving the need for welding techniques that are more efficient, precise, and environmentally friendly. Operational factors such as welding speed, current, voltage, and gas flow rate significantly influence the quality of weld joints. Therefore, the study focuses on using X-ray imaging to detect and analyze internal defects in welding methods is timely and relevant.

This study aims to systematically compare the effectiveness and quality of SMAW, MAG, and TIG welding methods in pipeline applications using X-ray imaging to detect and analyze internal defects. By examining the hidden imperfections in weld joints, this research seeks to provide evidence-based recommendations to improve welding practices, thereby reducing the incidence of defects and enhancing the reliability of pipeline systems in practical applications. The findings of this study are expected to contribute significantly to the field of welding technology, offering valuable understandings for industry professionals and researchers dedicated to advancing pipeline safety and performance.

Method and Materials

The methodology employed in this study was carefully chosen to ensure the accurate and reliable results in detecting weld defects in pipe welding. By utilizing X-Ray imaging, this study leverages advanced imaging technology to provide good insights into weld quality. The samples were tested by placing them between the radiation source and the film. The film is used in X-Ray tests as a recording medium. Both sides of the polyester film base are coated with a protective layer. This coating provides a transparent medium. The protective coating was applied to shield the film from external damage [12,13]. In the inspection process, a large beam of radiation is directed at the area of interest. This radiation passes through the area, and the resulting internal details are captured as cross-sectional images on a tomographic film, providing a comprehensive view of the internal structure.

This method stands out due to its precision, speed, and ease of identifying and interpreting defects, making it a superior choice for quality control in welding processes. The

comprehensive analysis of weld defects across three different welding techniques—MAG, TIG, and SMAW—enables a robust comparison, ensuring that the results are not only relevant but also actionable. This approach aligns with industrial standards and previous research, offering a systematic and reproducible methodology to enhance welding productivity, quality, and cost-efficiency.

Factors Affecting the Quality and Accuracy of Radiographic Results

The quality and accuracy of X-ray results in welding performance assessment are influenced by several variables and conditions. First, voltage and current must be appropriately set based on the material's thickness and type to generate sufficient X-rays for penetration without causing image distortion. Additionally, the optimum angle and position of the X-ray source relative to the weld are crucial for obtaining the best possible image. Furthermore, the radiation detector's sensitivity should range between 2-4% of the material thickness, while the exposure time must be calibrated to achieve clear and accurate images. Moreover, contrast agents can enhance image quality, making defects more visible. Specialized software is also used to analyze images and identify defects that may be challenging to detect with the naked eye. Finally, the personnel conducting the radiographic inspection must be qualified and certified according to international standards and specifications [14,15].

In previous studies, welding defects in a single welding process were addressed without comparing them to other welding methods for the purpose of quality control and process monitoring.

In this research, we investigate welding defects in three different pipe welding techniques using X-ray imaging testing, Figure 1.



Figure 1. X-ray radiographic testing machine

The reason for choosing this method for defect detection lies in its speed, accuracy, and ease of defect identification and result interpretation.

The resulting defects from the different welding processes will be evaluated according to X-ray acceptance and rejection criteria. Practical experiments will be conducted on a set of samples, followed by a discussion of the resulting defects, their causes, and methods

for preventing them. Now, more than ever, we need pipe welding processes that offer higher productivity, higher weld quality, lower cost, and manufacturing precision.

Welding Defects

Welding defects are generally classified into six groups according to the International Institute of Welding (IIW) classification system:

1.1.1. Group 100: Cracks

Cracks are linear discontinuities that can be either longitudinal (parallel to the weld axis) or transverse (perpendicular to the weld axis). Both types can significantly compromise the strength and integrity of the weld.

1.1.2. Group 200: Cavities

Various void defects can occur. Porosity, which consists of small gas pockets, weakens the weld and increases susceptibility to cracks. Cluster porosity, a severe concentration of gas bubbles, is a critical defect. Shrinkage cavities, which are voids from weld metal contraction, can occur on the surface or internally. Improper technique, moisture contamination, impurities, and solidification issues can all contribute to cavity formation.

1.1.3. Group 300: Solid Inclusions

This group includes various non-metallic impurities trapped within the weld: powder inclusions from incomplete flux removal, slag inclusions from trapped flux residue, tungsten inclusions from non-consumable electrodes, metallic oxide inclusions formed during welding, and other contaminants that can weaken the weld, promote stress cracking and corrosion, and reduce ductility.

1.1.4. Group 400: Incomplete Fusion and Penetration

Group 400 addresses incomplete fusion and penetration defects. Incomplete fusion occurs when the weld metal fails to fully merge with the base metal, creating weak points. Incomplete penetration happens when the weld metal doesn't fill the entire joint depth, reducing strength and introducing stress concentrations.

1.1.5. Group 500: Imperfect Shape

Group 500 addresses imperfections in weld shape. Undercut describes grooves along the weld edge due to insufficient fusion or penetration, weakening the weld and creating stress points. Overlap occurs when excess weld metal spills beyond the joint, affecting aesthetics and potentially introducing stress. Local protrusions are localized bulges caused by improper technique or excessive deposition, impacting functionality and creating stress concentrations.

1.1.6. Group 600: Miscellaneous Defects

It encompasses various defects. Excessive spatter creates a rough weld surface and safety hazards. Roughness can be caused by improper technique and increase corrosion. Porosity, cracks (which compromise structural integrity), and other defects like distortion can arise due to various factors and impact the weld's functionality, appearance, and strength [16].

Acceptance and Rejection Criteria for X-Ray Weld Defects According to ASME Standards

The X-ray imaging must cover at least 6mm on both sides of the weld line as a minimum requirement. Certain defects are categorically unacceptable, such as cracks and incomplete fusion. Other defects are subject to specific criteria to determine their acceptability.

Undercut defects are categorized into two types: surface and root. Surface undercuts are typically found at the edges, while root undercuts occur at the weld root. The acceptance criteria for undercuts are based on a 1 to 6 ratio. For example, if the weld length is 120mm, dividing by 6 gives 20mm, meaning any undercut exceeding 20mm is unacceptable.

For root concavity defects, the evaluation is based on the density or brightness in the film. If the root appears denser than the base metal, it is deemed unacceptable. Figure 2 illustrates the several types of weld defects visible in cross-sections and their expected appearances on radiographic images.

Other defects are assessed according to the following criteria:

- Any defect longer than 6mm is outright unacceptable.
- For samples with a thickness between 19mm and 57mm, the defect length should not exceed one-third of the sample's thickness.
- If multiple defects are close together, their total length must not exceed the sample's thickness.

Description	Radiogram	Weld Cross-Section
Gas Pore		
Linear Slag Inclusion		
Lack of Inter-run Fusion		
Longitudinal Fusion		
Porosity (linear)		
Lack of Root Fusion		
Radiating Cracks		
Traverse Crack		
Worm Hole		

Figure 2. The various types of weld defects observable in a cross-section and their expected appearances on radiographic images [17].

Experimental Work

1.1.7. Sample Preparation for Welding

A chemical analysis was conducted to determine the composition of the metal used for the pipes. The results are shown in Table 1.

From the table 1, it is clear that the carbon content is approximately 0.47%, indicating that the pipes are made of medium carbon steel, classified according to the American Iron and Steel Institute (AISI) as grade 1050.

Table 1. The chemical composition of the pipes (wt%)

Element	Silicon	Carbon	Manganese	Sulfur	Phosphorus	Aluminum	Copper	Iron
Percentage	0.468	0.229	0.761	0.0073	0.0285	0.0096	0.0005	98.45

A total of 36 pipe samples were prepared, each with a thickness of 6mm and a diameter of 170mm. Twelve samples were used for each welding process (MAG, TIG, SMAW), for a total of 6 samples per process. The samples were prepared and cut, with each pair of pieces beveled at a 30-degree angle. The samples were then thoroughly cleaned to remove external oxides and oils to ensure defect-free welding. Figure 3 illustrates the bevel angle, and Figure 4 shows the sample after preparation.

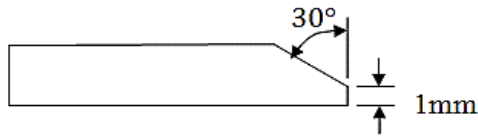


Figure 3. Beveling angle

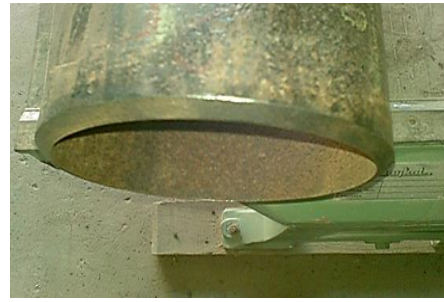


Figure 4. The sample after preparation

1.1.8. Welding processes

The 6G welding position, a specific technique for pipe welding, was utilized in this study. Figure 5 shows various pipe welding positions, and Figure 6 illustrates the position of one of the samples during the welding process.

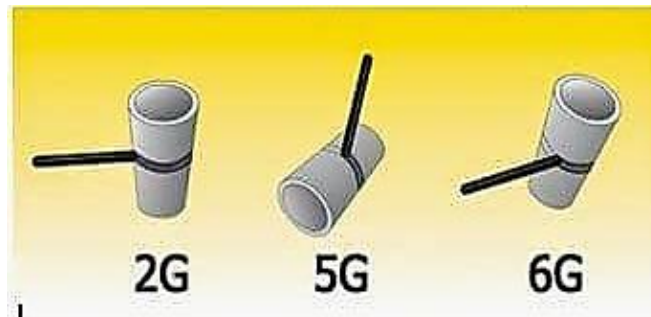


Figure 5. Common pipe welding positions



Figure 6. 6G welding position

SMAW Welding Process

The Shielded Metal Arc Welding (SMAW) process was conducted in three passes, each with different current settings. The first pass used a current of 55A with reverse polarity and an E6010 (2.5) electrode. The second pass used a current of 80A with an E7018 (2.5) electrode. The third pass used a current of 85A with the same electrode as the second pass. Grinding was performed after each welding pass.

MAG Welding Process

The Metal Active Gas (MAG) welding process was carried out in three passes at a constant voltage of 17V. The first pass was conducted with reverse polarity. The shielding gas used was a mixture of pure argon, carbon dioxide. The wire used had a 2901-A18 diameter of 0.8mm. The welds were ground after each pass.

TIG Welding Process

The Tungsten Inert Gas (TIG) welding process was performed in three passes. The first pass used a current of 80A, the second pass used 100A, and the third pass used 110A. No polarity reversal was applied in any of the passes. The tungsten electrode used had a SFA70 S3 diameter of 2.4mm.

It is worth noting that the welding parameters were selected according to industrial conditions and previous studies, taking into consideration the sample thickness.

X-Ray Assessment Process

The procedure for conducting the imaging process is shown in Figure 7 and summarized as follows:

The surfaces of the samples were thoroughly cleaned, especially in the weld area, prior to testing.

The X-ray device was positioned at a 45° angle.

The radiographic film was placed directly under the area to be inspected.

The distance between the film and the lens was set according to Table 2, following international standards.

Table 2. X-Ray Parameters and details

Test Sample l. D	varies
Size	$\varnothing 170mm, t = 6mm$
RT Technique	S.W.S.I
Curies/KV&Ma	170 KV,3Ma
Penetrated Thickness: mm	6 mm
Screen-Type & Thickness	Pb 2* .1 mm
Type of Film processing	MANUAL
Date Of Exam	2023\10\6
Material of manufacture	C/S
Focal Sopt/Source	3*3 mm
IQI Type & Designation	10 FEEN
Exposure Time	1.10 min
Extent Of Examination	100% WELD+HAZ
X-Ray & Serial No	88144 SMART ANDREX 225KV
Description of test sample	Pipe welding 6G
Manufacture Process	TIC, MAG, SMAW
Source/Film Distance	700 mm
Film – Type	D7
Developing Time	5 min
Test procedure	ASME V
Acceptance Criteria	ASME VIII

Figure 7 illustrates the X-ray machine and the 45° imaging angle used to avoid defect overlap in the film. In the attached image, the target area is the surface touching the ground, with the film placed underneath. The tube was rotated after each imaging process to ensure the entire weld line was captured, with each sample having three radiographic films taken.



Figure 7. X-ray machine and imaging angle at 45°

The study assumes that the sample size and welding conditions accurately represent typical industry practices. Operator skill levels and controlled environmental conditions may vary, potentially affecting the results. The focus on X-ray detectable defects may overlook other significant defects not visible with this method.

Furthermore, all experimental procedures adhered to industry standards and safety protocols, ensuring ethical conduct and minimizing environmental impact.

Results and Discussion

By examining the X-ray films and the report detailing the types of defects identified, a thorough review of the defects for each welding process was conducted. Figure 8 illustrates some of the defects identified across the three welding processes.

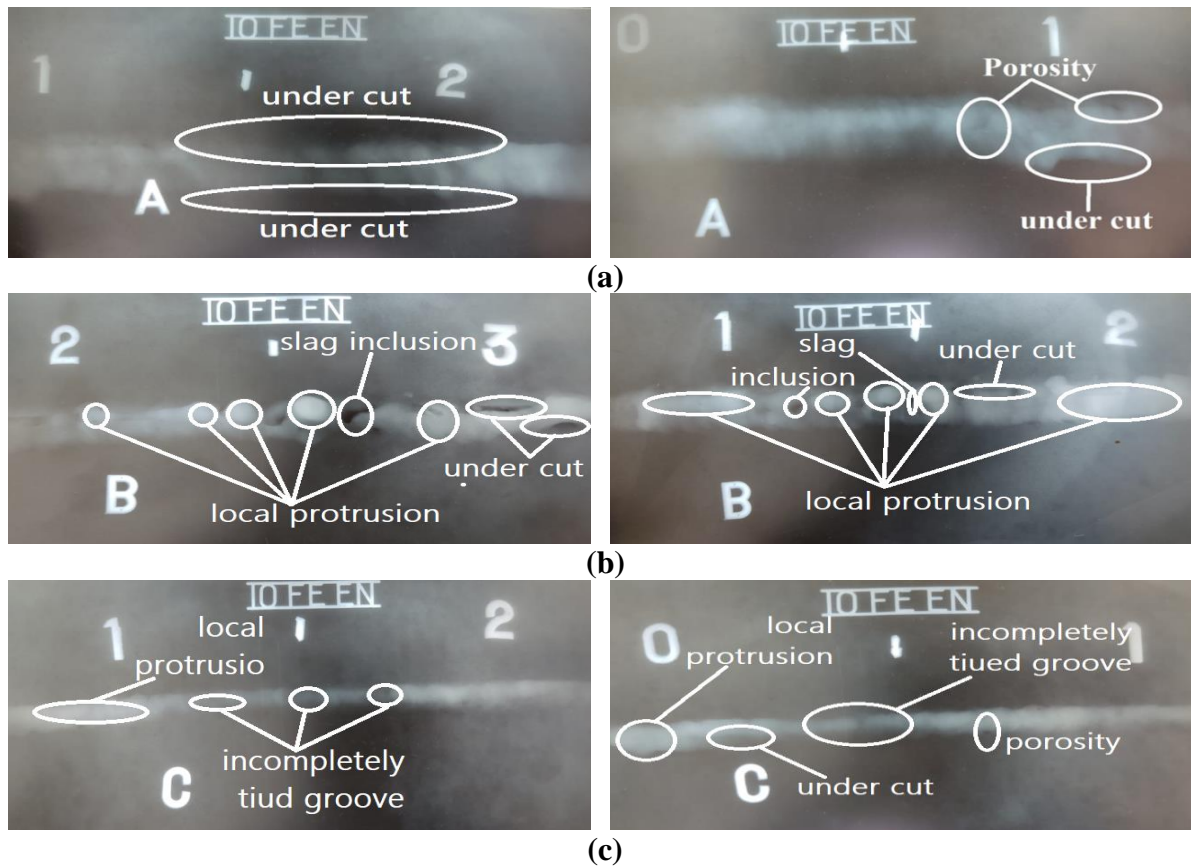


Figure 8. Some defects that have been discovered; (a) MAG, (b) SMAW, and (c) TIG

The identified defects among the sample, their acceptability, location within the sample, and their size are given in Table 3. various of welding defects were detected using X-ray imaging.

Table 3. The obtained results, detailing the identified defects, their acceptability, location within the sample, and their size.

Film No	EXAMINATION RESULT				
	Flaw Type	Flaw Size	Flaw Location	Weld Acc/Rej	Film Acc/Rej
T1	Tungsten Inclusion	1 mm	Middle	Acc	Acc
T1	Local protrusion	2mm	Spread	Acc	Acc
T1	Under cut	3mm	Spread	Acc	Acc
T1	Under cut	2mm	Spread	Acc	Acc
T1	Incompletely tiued groove	3mm	Middle	Rej	Acc
T1	Porosity	1mm	Edge	Acc	Acc
T2	Porosity	2mm-4mm	Spread	Acc	Acc
T3	Porosity	3mm	Edge	Acc	Acc
T3	Incompletely tiued groove	3mm	Edge	Rej	Acc
T3	Under cut	3mm	Edge	Acc	Acc
T3	Under cut	3mm	Edge	Acc	Acc
T3	Local protrusion	-----	Edge	Acc	Acc
T3	Tungsten Inclusion	1mm X 3	Edge	Rej	Acc
T4	-----	-----	-----	Acc	Acc
T5	-----	-----	-----	Acc	Acc
T6	-----	-----	-----	Acc	Acc
S1	Porosity	2mm	Edge	Acc	Acc
S1	Local protrusion	-----	Edge	Acc	Acc
S2	Porosity	2mm-4mm	Spread	Acc	Acc
S2	Slag inclusion	3mm	Edge	Acc	Acc
S3	Local protrusion	-----	Middle	Acc	Acc
S3	Local protrusion	7mm	Middle	Acc	Acc
S3	Slag inclusion	-----	Middle	Acc	Acc
S4	Porosity	1mm	Edge	Acc	Acc
S4	Slag inclusion	1mm	Edge	Acc	Acc
S5	-----	-----	-----	Acc	Acc
S6	-----	-----	-----	Acc	Acc
M1	Porosity	1mm	Middle	Acc	Acc
M1	Cluster Porosity	2mm-4mm	Middle	Rej	Acc
M2	Porosity	2mm	Edge	Acc	Acc
M2	Under cut	4mm	Edge	Acc	Acc
M2	Under cut	8mm	Middle	Acc	Acc
M2	Under cut	6mm	Middle	Acc	Acc
M3	Cluster Porosity	3mm-4mm	Edge	Rej	Acc
M3	Incomplete Penetration	7cm	all	Rej	Acc
M4	Porosity	2mm	Edge	Acc	Acc
M5	-----	-----	-----	Acc	Acc
M6	-----	-----	-----	Acc	Acc

To facilitate a comprehensive analysis, the defects were categorized and evaluated individually for each welding process. This approach allowed for a detailed comparison and assessment of the nature, frequency, and impact of the defects on weld quality. The

key findings are reported in Tables 4, 5 and 6 followed by insights gained from this evaluation are highlighted below.

Table 4. Defects Identified in TIG Welded Samples

Defect Type	Sample Number					
	1	2	3	4	5	6
Tungsten Inclusion	X					
Porosity	X	X	X			
Incomplete filled groove weld	X		X			
Under cut	X X		X X			
Local protrusion	X		X			

Table 5. Defects Identified in SMAW Welded Samples

Defect Type	Sample Number					
	1	2	3	4	5	6
Porosity	X	X		X		
Slag inclusion		X	X	X		
Local protrusion	X		X X			

Table 6. Defects Identified in MAG Welded Samples

Defect Type	Sample Number					
	1	2	3	4	5	6
Porosity	X	X		X		
Cluster Porosity	X		X			
Under cut		XXX				
Incomplete Penetration			X			

The X-ray inspection revealed a spectrum of defects across TIG, MAG, and SMAW welds, categorized by their type, location, and acceptability based on established criteria. The primary defects included incomplete penetration, cluster porosity, incomplete fusion, tungsten inclusions, porosity, undercut, localized protrusion, and slag inclusions.

TIG welding demonstrated the lowest defect frequency, with tungsten inclusions and incomplete fusion as primary concerns. Tungsten inclusions likely resulted from electrode contamination or improper shielding, while incomplete fusion indicated insufficient heat input or poor weld pool control. Porosity, commonly attributed to gas entrapment, was present but generally acceptable due to its limited size and distribution. SMAW welds were characterized by a higher frequency of slag inclusions and localized protrusions. Incomplete slag removal caused slag inclusions, and excessive heat input or improper travel angle often led to localized protrusions. Porosity was also present, similar to TIG welds. When the electrode retracts back and continues forward, this leads to the penetration of slag inside the melt.

MAG welding had the highest number of defects, with cluster porosity and incomplete penetration posing significant concerns. Turbulent weld pool conditions caused cluster porosity, while insufficient heat input or poor weld pool fusion led to incomplete penetration.

Overall, the X-ray analysis highlighted the critical influence of welding parameters, operator skill, and post-weld cleaning on weld quality. The presence of specific defects provides insights into potential root causes, such as inadequate shielding gas protection, improper electrode/filler wire manipulation, and suboptimal heat input. These findings emphasize the need for rigorous process control and continuous improvement to enhance weld integrity and reliability.

Conclusion

Through X-ray cross-sectional imaging of TIG, MAG, and SMAW weld samples, defects were detected and evaluated, distinguishing acceptable from rejected samples. In TIG welding, samples 1 and 3 were rejected due to significant defect concentrations, while samples 2, 4, 5, and 6 were accepted. Similarly, in SMAW welding, sample 3 was rejected, while samples 1, 2, 4, 5, and 6 were accepted. For MAG welding, samples 1, 2, and 3 were rejected, whereas samples 4, 5, and 6 were accepted.

Key observations include the absence of undercut defects in SMAW welding, highlighting this method's advantage. Grinding after each welding pass in SMAW and MAG processes was identified as a primary cause of defects when not completed or cleaned correctly.

Cluster porosity, a critical defect indicative of potential failure and collapse, was solely observed in MAG welding. Some samples were rejected due to concentrated defects, which may be individually acceptable, but multiple defects along the same welding path and at close distances increase the risk of failure and collapse.

This study simulated operational conditions and pipe use in the oil sector, emphasizing the essential role of welders [18]. Most defects were traced to welding angle faults and incorrect welding speed—either too slow or too fast.

Despite three rejected samples according to standards, MAG welding proved superior among the methods used for this pipe thickness. For thicknesses less than 6mm, TIG welding is preferred. The 6G welding position is noted as challenging, contributing to identified defects such as incomplete penetration and local protrusions.

Acknowledgment The authors gratefully acknowledge the Libyan Advanced Occupational Center for Welding Technologies for their facilitation of the experimental work presented in this study.

References

- [1] Ditchburn RJ, Burke SK, Scala CM. NDT of welds: state of the art. NDT&E International 1996;29(2):111–7

- [2] Bettayeb F, Benbartaoui H, Rouaroua B. The artificial intelligence in service of ultrasonic inspection reliability. Roma: 15th WCNDT; 2000.
- [3] Singh, R. (2021). Arc welding processes handbook. John Wiley & Sons.
- [4] Omiogbemi, I. M. B., Yawas, D. S., Dagwa, I. M., & Okibe, F. G. (2017). Effects of metal inert gas welding parameters on some mechanical properties of austenitic stainless steel in acidic environment. *Nigerian Journal of Technology*, 36(3), 835-843.
- [5] RHG e Silva, R. H. G., dos Santos Paes, L. E., Marques, C., Riffel, K. C., & Schwedersky, M. B. (2019). Performing higher speeds with dynamic feeding gas tungsten arc welding (GTAW) for pipeline applications. *Journal of the Brazilian Society of Mechanical Sciences and Engineering*, 41, 1-6.
- [6] Phillips, D. H. (2023). *Welding engineering: an introduction*. John Wiley & Sons.
- [7] Jastrzębski, R. (2015). Control of MIG/MAG welding machines. *Welding International*, 29(6), 454-456.
- [8] Fande, A. W., Taiwade, R. V., & Raut, L. (2022). Development of activated tungsten inert gas welding and its current status: A review. *Materials and manufacturing processes*, 37(8), 841.
- [9] Deepak, J. R., Raja, V. B., Srikanth, D., Surendran, H., & Nickolas, M. M. (2021). Non-destructive testing (NDT) techniques for low carbon steel welded joints: A review and experimental study. *Materials Today: Proceedings*, 44, 3732-3737.
- [10] I. D. Harris, "Welding advances in tube and pipe applications," *Welding Journal*, vol.90, no.6, pp.58-63, 2011.
- [11] Hu, A., Wu, L., Huang, J., Fan, D., & Xu, Z. (2022). Recognition of weld defects from X-ray images based on improved convolutional neural network. *Multimedia Tools and Applications*, 81(11), 15085-15102.
- [12] B. Chassignole, R. El Guerjouma, M.-A. Ploix, T. Fouquet, Ultrasonic and structural characterization of anisotropic austenitic stainless-steel welds: Towards a higher reliability in ultrasonic non-destructive testing, *NDT E Int.* 43 (4) (2010) 273–282, <https://doi.org/10.1016/j.ndteint.2009.12.005>.
- [13] T. Warren Liao, Jiawei Ni, An automated radiographic NDT system for weld inspection: Part I - Weld extraction, 1995
- [14] Kjelle, E., & Chilanga, C. (2022). The assessment of image quality and diagnostic value in X-ray images: a survey on radiographers' reasons for rejecting images. *Insights into Imaging*, 13(1), 36.
- [15] Withers, P. J., Bouman, C., Carmignato, S., Cnudde, V., Grimaldi, D., Hagen, C. K., ... & Stock, S. R. (2021). X-ray computed tomography. *Nature Reviews Methods Primers*, 1(1), 18.
- [16] Pan, H., Pang, Z., Wang, Y., & Chen, L. (2020). A new image recognition and classification method combining transfer learning algorithm and Mobilenet model for welding defects. *IEEE Access*, 8, 119951-119960.

- [17] British Standards Institution. (1998). Welding and allied processes—Classification of geometric imperfections in metallic materials—Part 1: Fusion welding (BS EN ISO 6520-1).
- [18] Saryanto, S., Purba, H. H., & Trimarjoko, A. (2020). Improve Quality Remanufacturing Welding and Machining Process in Indonesia Using Six Sigma Methods. *Journal European Des Systemes Automatises*, 53(3).